

Application of the node-centric indirect boundary element method to 3D multi-material rock problems

Sina Moallemi *, Thamer Yacoub & John H. Curran
Rocscience Inc., Toronto, Ontario, Canada

ABSTRACT: An indirect formulation for the boundary element method (BEM) has been used in a variety of linear elastic infinite domains containing joints, faults, and excavations. The displacement discontinuity (DD) method is employed to describe the behaviour of joints, while the boundaries of excavations and tunnel surfaces are modeled by fictitious elements. In this work, the node-centric indirect BEM is employed, where linear triangular elements are used to discretize the domain, and nodes are assigned to the corner of each element. In this paper, the application of this approach is extended for multi-material domains, where a double-layer element is defined on the material boundaries. This method captures the behaviour of each zone independently of the rest of the domain and is compared with several numerical and analytical methods and found to be in good agreement.

1 INTRODUCTION

There are two approaches for solving the equilibrium equation in an elastic domain using the BEM: direct and indirect. In the *direct* formulation, an appropriate Dirac-Delta function is used, and the weak form of the equilibrium equations is derived by employing the divergence theorem. In contrast, the *indirect* formulation uses a singular solution that satisfies the governing equations over the boundaries of interest, such as the free-space Green functions (Banerjee and Butterfield, 1981). In this paper, the indirect formulation is used to calculate the stresses and displacements on the surface as well as at any point within the domain. Geomechanics software has typically been based on *constant* indirect element formulations. However, with constant elements, a fine mesh is required to obtain high accuracy near the boundary (Beer and Watson, 1992). To overcome this issue, Vijaykumar et al. (2000) introduced the general *node-centric* method, which provides a higher degree of accuracy using a lower number of elements. In the node-centric method, a linear triangular element is defined, and the nodes are placed at the corners of each element. This technique not only satisfies the continuity of displacements and stresses along the surface, but also accounts for the variation of unknowns within an element. To generalize this method, a special integration algorithm was introduced that captures the singular and near-singular cases (Vijaykumar et al., 2000).

In this paper, we extend the node-centric indirect method to 3D multi-material rock problems. Hence, we create a set of double-layer elements on each material boundary to satisfy the equilibrium equation and the continuity of displacements along the boundary. We verify the new approach with several examples, and the results are in good agreement with the analytical solution and other numerical methods.

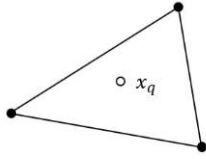
2 METHODOLOGY

In this section, we give a brief overview of the mathematical formulation of node-centric indirect BEM and present the special integration required to capture the singular cases (Yacoub, 1998). We then discuss in detail the proposed approach for modeling the multi-material domain.

2.1 Mathematical formulation

Proposing the use of a general indirect BEM in geomechanical problems requires capturing two behaviour in the domain, one dedicated to displacement discontinuities in rock joints and the other to continuities in the response of material boundaries, such as tunnel surfaces. Deriving a mathematical framework for each of these cases requires a single solution that calculates the displacement field (\mathbf{u}) at interest point (x_q) owing to an applied concentrated load (\mathbf{e}) at any point within the domain (x_p), as shown in Figure 1 below, that can be written as:

$$u_i(x_p) = B_{ij}(x_p, x_q) e_j(x_q) \quad (1)$$



x_p

Figure 1. Schematic position of the interest point x_p and the triangular element

Here, B_{ij} is the second order tensor and is calculated for both the formulation of indirect DD and fictitious cases (Banerjee and Butterfield, 1981, and Vijayakumar et al., 2000). By obtaining the displacement field, strain and stress can be presented as:

$$\varepsilon_{ij}(x_p) = \frac{1}{2} \left(\frac{\partial u_i}{\partial x_j} + \frac{\partial u_j}{\partial x_i} \right) = H_{ijk}(x_p, x_q) e_k(x_q) \quad (2)$$

By applying Hook's law, one can write:

$$\sigma_{ij}(x_p) = D_{ijkl} \varepsilon_{kl}(x_p) = G_{ijk}(x_p, x_q) e_k(x_q) \quad (3)$$

where σ_{ij} is the stress tensor, D_{ijkl} is the fourth-order tangential stiffness operator tensor, and the third-order tensor G is the Green function (Crouch and Starfield, 1983). In addition, the traction on the surface t_i with the normal direction n , as shown in Figure 2, can be obtained by using Equation (3) as:

$$t_i(x_p) = \sigma_{ij} n_j = K_{ij}(x_p, x_q) e_j(x_q) \quad (4)$$

In a discretized domain, instead of a concentrated point load $\mathbf{e}(x_p)$, we can assume its linear variation over the triangular element, i.e., $e_i(x) = \sum N_k(x) \bar{\varphi}_i^k$, where N is the linear shape function associated with each node and $\bar{\varphi}_i^k$ can be interpreted as the i^{th} fictitious component associated with the k^{th} nodal concentrated force of each element.

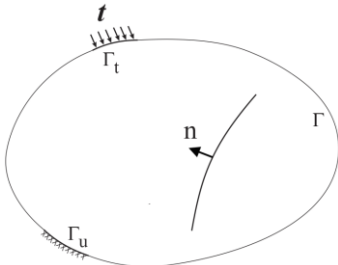


Figure 2. Different boundaries of the domain

By applying the above relation to Equations (1) and (4), one can obtain displacement and traction as:

$$u_i(x_p) = \sum_{e=1}^n \left(\int_{\Gamma} B_{ij}(x_p, x_q) N_k \bar{\varphi}_j^k d\Gamma \right), \quad t_i(x_p) = \sum_{e=1}^n \left(\int_{\Gamma} K_{ij}(x_p, x_q) N_k \bar{\varphi}_j^k d\Gamma \right) \quad (5)$$

in which Γ defines the boundaries of the domain.

Consequently, in a numerical perspective, according to the traction and field points applied to the domain and the boundary conditions of the problem, we can use the matrix form of the above relation to obtain the unknown nodal values $\bar{\varphi}$. By calculating the unknowns, displacement at any point in the domain and on the boundaries can be found by using the first relation of Equation (5) above. It should be noted that taking the integration of Equation (5) requires special techniques such that Green's functions are unbonded at a singular point. While the point located at x_p has enough distance from the element surface, the integration can be performed with an appropriate number of gauss points. However, if the point is in a close distance from the element (near-singular case) or located exactly on the edge or the surface of the element (singular case), an innovative numerical technique, proposed by Vijayakumar and Cormack (1989), is applied to calculate the integration. In this method, for the singular or near-singular conditions, by employing the divergence theory, the integration over the area of an element would be transformed to the edges of the elements. As explained by Vijaykumar et al. (2000), by applying this methodology to Equation (5), displacement and traction would be represented by a set of boundary functions instead of by Green functions as introduced earlier.

2.2 Modeling of multi-material domains

As mentioned above, Equation (5) is presented for an infinite homogenous elastic medium. However, modeling multi-material domains is unavoidable in geomechanics. In this paper, a new formulation of the node-centric BEM is presented to model multi-material domains. Let's consider the domain shown in Figure 3(a) below, containing two different material zones with associated material properties. The normal direction of elements in each zone is facing inward. The basic assumption here is that the continuity of material boundaries, i.e., the total displacement, is the same on the boundaries of the zones, hence, the fictitious elements are used to define material boundaries. In addition, due to equilibrium, the summation of tractions on the boundary surfaces is assumed to be zero.

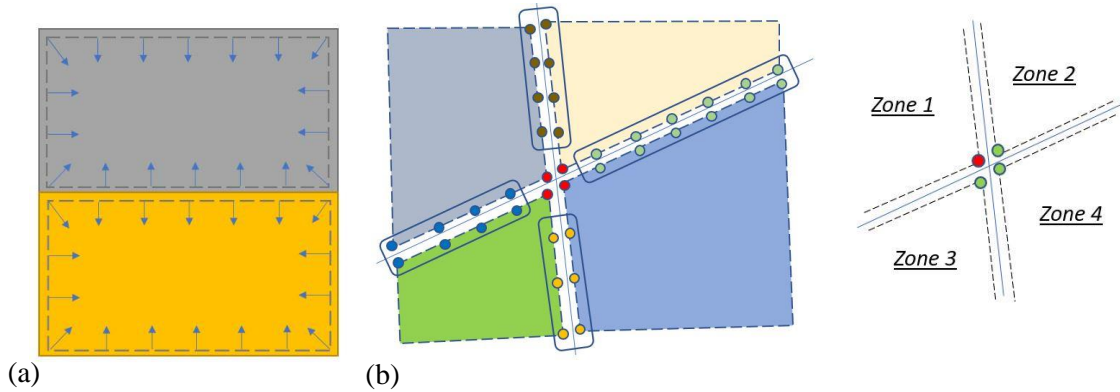


Figure 3. (a) Double-layered element on the boundary, (b) Master-slave nodes at the corner of a multi-material domain

Consequently, for any node on the boundary, there is a conjugate node in an adjacent zone. By assuming one of these nodes as master (superscript m) and the other one as slave (superscript s), one can write:

$$u_i^m - u_i^s = 0, \quad t_i^m + t_i^s = 0 \quad (6)$$

noting that both u_i and t_i are given in Equation (5). The above relation can be applied only to the nodes on the material boundary surfaces. However, Equation (5) would be applied to the rest of the nodes of each zone. In a schematic view, the final form of stiffness matrix for the domain given in Figure 4 below (Banerjee and Butterfield, 1981) can be presented as:

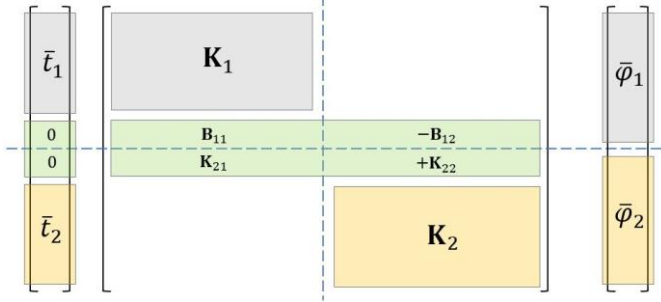


Figure 4. Matrix form for solving system of equations in bi-material domain

In general, multiple zones might intersect, as shown in Figure 3(b). As can be seen, for the nodes on the corner, there is not a unique conjugate node to satisfy Equation (6) above. Therefore, this relation should be modified to handle this type of problem. In this case, one of the nodes on the corner is assumed to be a master node, and the rest are considered slave nodes. Since the displacement for all these nodes are the same, we have:

$$u_i^m - u_i^{s(j)} = 0, \quad (j = 1 \text{ to } n_s) \quad (7-a)$$

where n_s is the total number of slave nodes. On the other hand, with regard to equilibrium, the summation of all traction at this point is assumed to be zero, i.e.,

$$t_i^m + \sum_{j=1}^{n_s} t_i^{s(j)} = 0 \quad (7-b)$$

The accuracy of this methodology is presented in the following section through comparison with examples of several numerical and analytical methods

3 NUMERICAL INVESTIGATION

3.1 Tunnel in a three-layered soil

The first example is a model of a tunnel in a three-layered soil under confining field stress, as shown in Figure 5(a) below. This example was presented by Shou and Napier (1999) to investigate the stress distribution around the tunnel for five different cases. In the first case, the tunnel is surrounded by two weak layers where the module of elasticity of the middle layer, E_2 , is 100 times greater than the other layers. However, in the last case, the middle layer is the weaker one, in which $E_1/E_2=0.01$. In the following, the ratios of material properties are given for all cases:

- | | |
|-----------------------------------|----------------------------------|
| <i>Case1</i> : $E_1 / E_2 = 100$ | <i>Case2</i> : $E_1 / E_2 = 10$ |
| <i>Case3</i> : $E_1 / E_2 = 1.0$ | <i>Case4</i> : $E_1 / E_2 = 0.1$ |
| <i>Case5</i> : $E_1 / E_2 = 0.01$ | |

The radius of the tunnel is assumed to be 1.0 m, the distance from the tunnel's center to the top layer (c) 2.0 m, and the module of elasticity of the middle layer 50GPa.

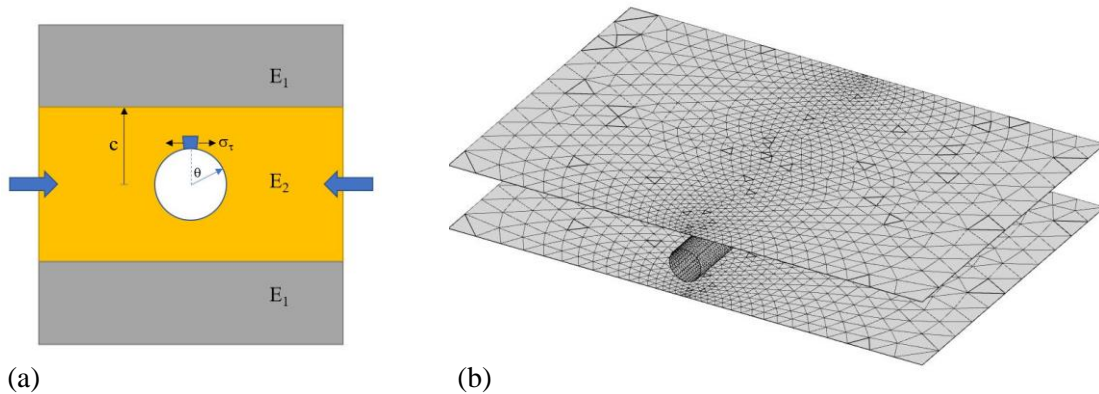


Figure 5. (a) Geometry of tunnel in soil, (b) 3D surface mesh used in BEM

The 3D mesh used for the BEM simulation is provided in Figure 5(b). The top and bottom layers are defined as double-layered elements in order to define the material boundaries. The horizontal field stress is applied to the domain and the normalized tangential stress around the tunnel is calculated. The obtained results are plotted in Figure 6 below and compared with the proposed results by Shou and Napier (1999), showing very close agreement. In Figure 6, the results calculated by the BEM are shown with a marker and the given results from literature are shown with a line. It can be observed that a higher tangential stress is obtained where the surrounding layers are stronger while, for the case of weaker layers around the tunnel, lower tangential stress is as expected.

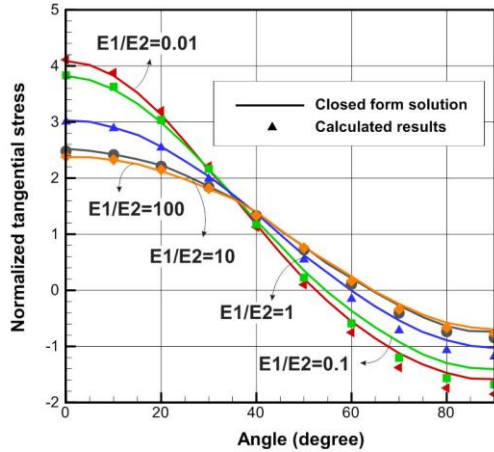


Figure 6. Variation of tangential stress around the tunnel in different angles for all five cases.

3.2 Settlement in a multi-layered soil

In the second example, the settlement of a three-layered soil under surface traction is examined. The geometry of the example is given in Figure 7(a) below. The stiffness of the top to bottom layers are 50, 30, and 10 MPa, respectively. There is a circular footing with the radius of 5m, and the magnitude of 1MPa is applied on the surface.

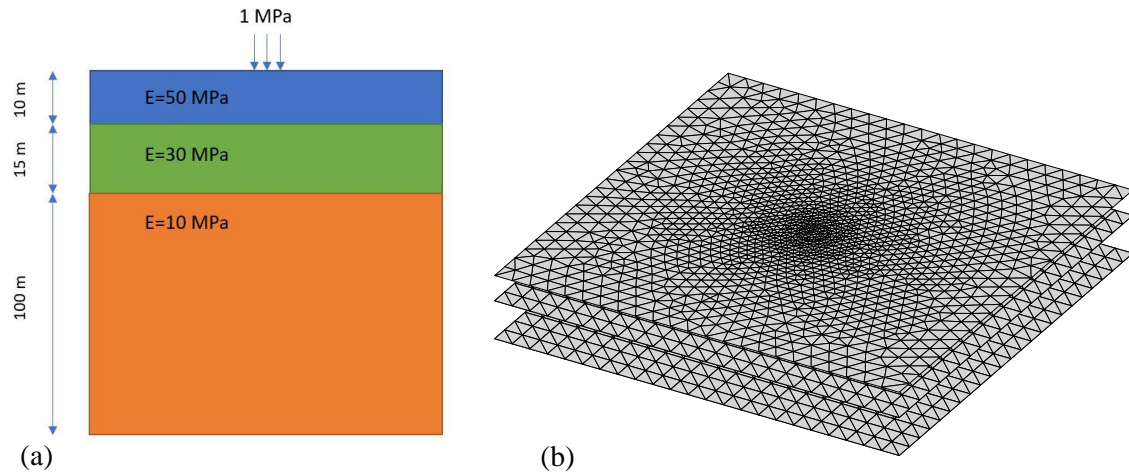


Figure 7. (a) Geometry of the three-layered soil, (b) 3D surface mesh used in BEM analysis

The total deformation is compared with the results obtained by Boussinesq's solution for multi-material domain provided in *Settle* software. The 3D surface mesh for the ground and boundary layers are given in Figure 7(b). According to the external load applied to the surface, the unknown nodal values $\bar{\varphi}$ can be obtained. By finding these unknowns, the displacement on the surface and at any arbitrary field point can be calculated. In Figure 8(a), the vertical displacement is presented under the applied load. As can be seen, the continuity of deformation between layers is satisfied.

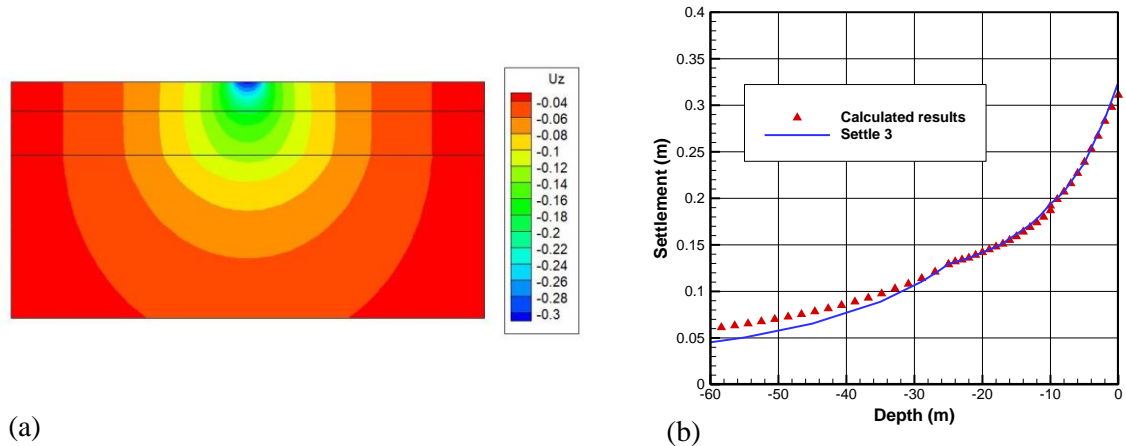


Figure 8. (a) Vertical displacement on field point in three layers, (b) Variation of vertical deformation and comparison with *Settle* software

To compare the accuracy of the results, the vertical displacement beneath the loading surface is determined for the proposed technique and *Settle* software, as plotted in Figure 8(b) above. As can be seen, very similar results are obtained, which demonstrates the ability of the node-centric BEM to solve multi-material domains.

4 CONCLUSION

In this paper, the indirect node-centric BEM has been formulated to solve the multi-material elastic domains. In this technique, double-layered elements are introduced on the material boundaries while the normal directions are pointing to their relevant zones. By incorporating the continuity of displacement and satisfying the equilibrium for the nodes on double-layered elements to the general equilibrium equation, the stress distribution and deformation in the domain were obtained. Since the elements in node-centric methods are sharing nodes, the results are assumed to be smooth and averaging is not required, which leads to more accurate results and saves computational time on calculation of the matrix. The accuracy of the proposed technique was examined through comparison with other numerical methods, and very similar results were obtained. This makes the indirect node-centric BEM technique a very good candidate for solving 3D elastic domains.

REFERENCES

- Banerjee, P.K., Butterfield, R. 1981. *Boundary element methods in engineering science*. England: McGraw-Hill.
- Beer, G., Watson, J.O. 1992. *Introduction to finite element and boundary element methods for engineers*. England: Wiley.
- Crouch, S.L., Starfield, A.M. 1983. *Boundary element methods in solids mechanics with applications in mechanics and geological engineering*. London: George Allen and Unwin.
- Shou, K., Napier, J.A.L. 1999. A two-dimensional linear variation displacement discontinuity method for three-layered elastic media. *International Journal of Rock Mechanics and Mining Science* 36: 719-729.
- Vijayakumar, S., Cormack, D.E. 1989. A new concept in near-singular integral evaluation: the continuation approach. *Society for Industrial and Applied Mathematics* 49: 1285-1295.
- Vijayakumar, S., Yacoub, T.E., Curran, J.H. 2000. A node-centric indirect boundary element method: three-dimensional displacement discontinuities. *Computers and Structures* 74: 687-703.
- Yacoub, T.E. 1998. *Three-dimensional analysis of lenticular ore bodies using displacement discontinuity elements*. Ph.D. Thesis: University of Toronto.